

## Two universality classes of the Ziff-Gulari-Barshad model with CO desorption via time-dependent Monte Carlo simulations

Henrique A. Fernandes,<sup>1</sup> Roberto da Silva,<sup>2</sup> and Alinne B. Bernardi<sup>1</sup>

<sup>1</sup>*Instituto de Ciências Exatas, Universidade Federal de Goiás, Regional Jataí, BR 364, km 192, 3800-CEP 75801-615, Jataí, Goiás, Brazil*

<sup>2</sup>*Instituto de Física, Universidade Federal do Rio Grande do Sul, Av. Bento Gonçalves, 9500-CEP 91501-970, Porto Alegre, Rio Grande do Sul, Brazil*



(Received 20 April 2018; published 11 September 2018)

We study the behavior of the phase transitions of the Ziff-Gulari-Barshad (ZGB) model when CO molecules are adsorbed on a catalytic surface with a rate  $y$  and desorbed from the surface with a rate  $k$ . We employ large-scale nonequilibrium Monte Carlo simulations along with an optimization technique based on the coefficient of determination, in order to obtain an overview of the phase transitions of the model in the whole spectrum of  $y$  and  $k$  ( $0 \leq y \leq 1$  and  $0 \leq k \leq 1$ ) with precision  $\Delta y = \Delta k = 0.001$ . Successive refinements reveal a region of points belonging to the directed percolation universality class, whereas the exponents  $\theta$  and  $\beta/\nu_{\parallel}$  obtained agree with those of this universality class. On the other hand, the effects of allowing the CO desorption from the lattice on the discontinuous phase transition point of the original ZGB model suggest the emergence of an Ising-like point previously predicted by Tomé and Dickman [*Phys. Rev. E* **47**, 948 (1993)]. We show that such a point appears after a sequence of two lines of pseudocritical points which leads to a unique peak of the coefficient of determination curve in  $y_c = 0.554$  and  $k_c = 0.064$ . In this point, the exponent  $\theta$  agrees with the value found for the Ising model.

DOI: [10.1103/PhysRevE.98.032113](https://doi.org/10.1103/PhysRevE.98.032113)

### I. INTRODUCTION

Over several decades, the study of the critical behavior of many-body systems has been mainly carried out through Monte Carlo simulations, which makes it one of the most important methods in statistical mechanics. At the very beginning, to circumvent the critical slowing down (characteristic of the long-time regime) of systems close to their critical point was not a simple task. However, nowadays, with the advances in computational technology and with the discovery of new techniques, this is not the main concern anymore when studying phase transitions and critical phenomena of those systems. In 1989, Janssen *et al.* [1] and Huse [2] proposed a method which avoids the critical slowing down and is known as short-time (nonequilibrium) Monte Carlo (MC) simulations. They discovered, by using renormalization group techniques and numerical calculations, respectively, that there is universality and scaling behavior even at the early stage of the time evolution of dynamical systems [3]. Since then, this method has been successfully applied to a wide variety of problems ranging from systems with a defined Hamiltonian [4–21] to models based on generalized Tsallis statistics [22], protein folding models [23], and models without a defined Hamiltonian such as polymers [24], a contact process and cellular automaton [25], epidemic models [26], driven lattice gases [27], model of liquids [28,29], and even surface reaction models [30,31]. (An interesting review on the progress of this method was published by Albano *et al.* [32].)

The surface reaction models [33–36] have attracted considerable interest, whereas they possess phase transitions and critical phenomena and can be used to explain several experimental observations in catalysis [37–39]. One such model

was proposed in 1986 by Ziff *et al.* [40] to describe some nonequilibrium aspects of the catalytic reaction of carbon monoxide molecules (CO) and oxygen atoms (O) on a surface to produce CO<sub>2</sub> molecules, CO<sub>2</sub> (CO + O → CO<sub>2</sub>). In this model, also known as the ZGB model, the surface is represented by a two-dimensional regular square lattice. Both CO and O<sub>2</sub> molecules in the gas phase impinge the surface at rates  $y$  and  $1 - y$ , respectively. Each CO molecule which impinges the surface needs only one vacant site to be adsorbed on it. However, the O<sub>2</sub> molecule dissociates into two O atoms during its adsorption process. The atoms are both adsorbed on the surface when there exist two vacant nearest-neighbor sites. The production of CO<sub>2</sub> molecules occurs when, after the adsorption processes, a nearest-neighbor pair of CO and O is found. In this case, the CO<sub>2</sub> molecule desorbs and returns to the gas phase, leaving the surface with two vacant sites. This model possesses only one control parameter, the CO adsorption rate  $y$  (the partial pressure of CO in the gas phase), and exhibits three distinct states and two irreversible phase transitions: one continuous and another discontinuous. The continuous phase transition occurs at  $y = y_1 \sim 0.3874$  [41] and separates the O poisoned state ( $0 \leq y < y_1$ ) from the reactive state ( $y_1 < y < y_2$ ) where both CO and O and vacant sites coexist on the catalytic surface, and there is sustainable production of CO<sub>2</sub> molecules. The discontinuous phase transition occurs at  $y = y_2 \sim 0.5256$  [42] and separates the reactive state from the CO poisoned state ( $y_2 < y \leq 1$ ). So, despite the simplicity of this model, its rich phase diagram, experimental observations, and industrial applications have made the ZGB model one of the most prominent examples in the study of reaction processes on catalytic surfaces [43–45,47]. Several modified versions of the model have been

proposed in order to obtain more realistic systems of actual catalytic processes, for instance, by including CO desorption [46–56], diffusion [37,47,54–57], impurities [52,56,58–60], attractive and repulsive interactions between the adsorbed molecules [56,61], surfaces of different geometries [43,62], hard oxygen boundary conditions [63], etc.

The ZGB model has been studied with several techniques. One of them was considered recently by the authors and will be employed in this work to study the ZGB model with desorption of CO molecules. In that work [31], we studied the original ZGB model through short-time MC simulations and considered a method which is based on optimization of the coefficient of determination of the order parameter. In this way, it was possible to locate its nonequilibrium phase transitions. This amount, which measures the quality of a linear fit, is widely employed in statistics and was proposed for the first time in statistical mechanics by one of the authors of this work and other collaborators in order to optimize the critical temperature of spin systems [22]. Since then this method has been successfully applied to other systems with and without a defined Hamiltonian (see, for example, Refs. [17–19,21,26]).

As shown in Ref. [31], this method was able to characterize the continuous phase transition of the original ZGB model and its upper spinodal point, as well as estimate the static and dynamic critical exponents which are in complete agreement with results found in the literature.

By taking into consideration those unambiguous results, we decided to study a modified version of the ZGB model to include the desorption of CO molecules [46,49,50,55] from the catalytic surface in order to obtain a detailed structure of the phase diagram of the model. We do not consider the desorption of O molecules, whereas it has been shown that the desorption rate  $k$  of CO molecules is much higher than that of O atoms [37]. Physically, the desorption of CO molecules can be thought of as the temperature effect, which is a very important parameter in catalytic processes. In addition, the desorption of CO molecules from the surface also prevents the appearance of the CO poisoned phase, which turns the discontinuous phase transition reversible [51,52]. Although thinking of the desorption of CO molecules as an effect of temperature, in this work we do not include other correlated effects such as the diffusion of CO molecules and/or O atoms on the surface since we are concerned only with the analysis of the ZGB model with the desorption process. So this model has now two control parameters, the CO adsorption rate  $y$  and the CO desorption rate  $k$ . Our results show that the model possesses two universality classes: the directed percolation (DP) universality class in the region of the continuous phase transition of the original model, as well as a single point that apparently has Ising-like characteristics as suggested by Tomé and Dickman [46].

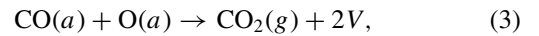
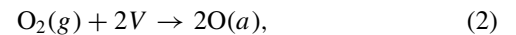
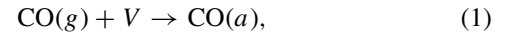
The rest of this paper is organized as follows. In Sec. II we present the modified version of the ZGB model to include the desorption of CO molecules from the surface and describe the short-time MC simulations as well as the technique known as coefficient of determination (see, for example, Ref. [64]). In Sec. III we present our main results by showing how these techniques can be used to obtain the phase diagram of the model. In that section, as additional results, we also estimate some critical exponents for some specific

critical points  $(y_c, k_c)$ . Finally, a brief summary is given in Sec. IV.

## II. MODEL AND SIMULATION METHOD

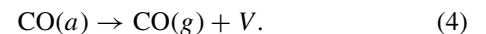
The ZGB model [40] simulates the catalytic oxidation obtained with the reaction between CO molecules and O atoms on a surface which, in turn, is in contact with a gas phase composed of CO and O<sub>2</sub> molecules.

This catalytic surface can be modeled as a regular square lattice, and its sites might be occupied by CO molecules or O atoms or may be vacant ( $V$ ). The reactions presented in the previous section follow the Langmuir-Hinshelwood mechanism [40,65] and are schematically represented by the following reaction equations:



where  $g$  and  $a$  refer, respectively, to the gas and adsorbed phases of the atoms and molecules. Equation (1) takes into account the adsorption process of CO molecules on the surface, i.e., if a CO molecule is selected in the gas phase (with a rate  $y$ ), a site on the surface is chosen at random, and, if it is vacant  $V$ , the molecule is immediately adsorbed at this site. Otherwise, if the chosen site is occupied, the CO molecule returns to the gas phase and the trial ends. Equation (2) considers the adsorption process of O<sub>2</sub> molecules, i.e., if an O<sub>2</sub> molecule is selected in the gas phase (with a rate  $1 - y$ ), then a nearest-neighbor pair of sites is chosen at random. If both sites are empty, the O<sub>2</sub> molecule dissociates into a pair of O atoms which are adsorbed on these sites. However, if one or both sites are occupied, the O<sub>2</sub> molecule returns to the gas phase and the trial ends. Finally, after each adsorption event, all nearest-neighbor sites of the newly occupied site are checked randomly. If one O-CO pair is found, they react immediately, forming a CO<sub>2</sub> molecule, which desorbs, leaving behind two vacant sites [Eq. (3)].

In this work, we modified the ZGB model by including the desorption of CO molecules with a rate  $k$  whose equation is given by



This equation accounts for the possibility, observed in experiments, of the desorption of CO molecules adsorbed on the catalytic surface without reacting. As pointed out above, we do not consider the desorption of O atoms since, as shown in Ref. [37], its desorption rate is much smaller than  $k$ .

Here the order parameter of the model is given by the density of vacant sites, which is defined as

$$\rho(t) = \frac{1}{L^d} \sum_{i=1}^{L^d} s_i, \quad (5)$$

where  $s_i = 1$  when the sites  $i$  are vacant; otherwise it is equal to zero.

The study is carried out via short-time MC simulations in order to obtain the phase diagram of the model. To perform the numerical simulations, we take into consideration that,

for systems with absorbing states, the finite size scaling near criticality can be described by the following general scaling relation [66]:

$$\langle \rho(t) \rangle \sim t^{-\beta/\nu_{\parallel}} f[(y - y_c)t^{1/\nu_{\parallel}}, t^{d/z}L^{-d}, \rho_0 t^{\beta/\nu_{\parallel} + \theta}], \quad (6)$$

where  $\langle \dots \rangle$  stands for the average on different evolutions of the system,  $d$  is the dimension of the system,  $L$  is the linear size of a regular square lattice, and  $t$  is the time. The indexes  $z = \nu_{\parallel}/\nu_{\perp}$  and  $\theta = \frac{d}{z} - \frac{2\beta}{\nu_{\parallel}}$  are dynamic critical exponents, and  $\beta$ ,  $\nu_{\parallel}$ , and  $\nu_{\perp}$  are static ones. Here  $y - y_c$  is the distance of a point  $y$  to the critical point,  $y_c$ , which governs the algebraic behaviors of the two independent correlation lengths: the spatial one,  $\xi_{\perp} \sim (y - y_c)^{-\nu_{\perp}}$ , and the temporal one,  $\xi_{\parallel} \sim (y - y_c)^{-\nu_{\parallel}}$ .

The critical exponents of the model can be estimated through Eq. (6) and from nonequilibrium MC simulations by taking into account three different initial conditions at criticality. When all sites of the lattice are initially vacant (with initial density  $\rho_0 = 1$ ), it is expected that the density of vacant sites decays algebraically as

$$\langle \rho(t) \rangle \sim t^{-\beta/\nu_{\parallel}} = t^{-\delta}, \quad (7)$$

and when the simulation starts with all sites filled with CO molecules ( $\rho_0 = 0$ ), or with O atoms, except for a single empty site located in the center of the lattice, i.e.,  $\rho_0 = 1/L^2$ , we expect

$$\langle \rho(t) \rangle \sim \rho_0 t^{\frac{d}{z} - 2\frac{\beta}{\nu_{\parallel}}} = \rho_0 t^{\theta}. \quad (8)$$

So the exponents  $\delta$  and  $\theta$  are given by the slope of the power laws in  $\log \times \log$  scale, respectively.

The algebraic behavior presented above along with other power laws found at the critical point (see, for example, Refs. [25,31]), both obtained via the short-time MC method, allows us to find the whole set of critical exponents of the model without the problem of critical slowing down. So, instead of waiting the system to achieve the steady state to perform the statistics, which in turn takes between  $10^4$  to  $10^8$  MC steps depending on the lattice size and other parameters, we consider only a few hundreds of MC steps at the beginning of the time evolution of dynamical systems to obtain our estimates. In addition, this technique also is used to estimate the critical points, whereas Eqs. (7) and (8) hold only at the criticality. So, out of criticality, those equations are not straight lines in  $\log$ - $\log$  scale. This is the main reason for the use of the coefficient of determination to estimate the critical points of the model. This coefficient is given by

$$r = \frac{\sum_{t=N_{\min}}^{N_{\text{MC}}} [\overline{\ln \langle \rho(t) \rangle} - a - b \ln t]^2}{\sum_{t=N_{\min}}^{N_{\text{MC}}} [\overline{\ln \langle \rho(t) \rangle} - \ln \langle \rho \rangle(t)]^2}, \quad (9)$$

where  $N_{\text{MC}}$  is the number of MC steps,  $\rho(t)$  is obtained for each pair of the control parameters of the model  $(y, k)$ ,  $a$  is the intercept and  $b$  the slope of a linear function,  $\overline{\ln \langle \rho(t) \rangle} = (1/N_{\text{MC}}) \sum_{t=N_{\min}}^{N_{\text{MC}}} \ln \langle \rho \rangle(t)$ , and  $N_{\min}$  is the number of MC

steps discarded at the beginning (the first steps). The coefficient  $r$  has a very simple interpretation: it is the ratio (expected variation)/(total variation) and ranges from 0 to 1. So the bigger the  $r$  ( $r \simeq 1$ ), the better the linear fit in  $\log \times \log$  scale, and therefore, the better the power law which corresponds to the critical point  $(y_c, k_c)$ . On the other hand, when the system is out of criticality, there is no power law and  $r \simeq 0$ . Thus, we can obtain the coefficient of determination for several pairs  $(y, k)$  by using, for instance, Eq. (7) or (8).

In this work, we consider Eq. (7) and obtain the coefficient of determination  $r$  for  $10^6$  pairs  $(y, k)$ , i.e., we perform simulations in the whole spectrum of values of  $y$  and  $k$  ( $0 \leq y \leq 1$  and  $0 \leq k \leq 1$  with  $\Delta y = \Delta k = 0.001$ ) in order to have a structure of the phase diagram of the model, as well as a clue of what happens with the continuous and discontinuous phase transitions of the original model when CO desorption is allowed.

### III. RESULTS

In this section, we present our main results by using large-scale short-time MC simulations. First, we consider the coefficient of determination to obtain the phase diagram of the model. The results allow us to observe in detail the changes caused by the inclusion of the CO desorption in the original ZGB model obtaining in this way its possible critical points  $(y_c, k_c)$ . With these points in hand, we estimate some critical exponents and compare our results with those ones found in the literature.

#### A. Coefficient of determination

Figure 1(a) shows the phase diagram of the ZGB model with CO desorption obtained through the coefficient of determination  $r$  given by Eq. (9) and by taking into consideration Eq. (7). To construct this figure, we needed to perform  $10^6$  independent simulations. Each simulation was carried out on square lattices of linear size  $L = 80$  with periodic boundary conditions and returned the value of  $r$  obtained for a given set of the control parameters,  $y$  and  $k$ . Here we considered the system starting with a lattice fully occupied by CO molecules, which means  $\rho_0 = 0$  since we are using the density of empty sites as the order parameter of the model. Each value of  $r$  is an average taken over 1000 samples in their first 300 MC steps without taking into account the first  $N_{\min} = 100$  MC steps. As stated above,  $r$  ranges from zero (black points), which means that the considered point  $(y, k)$  is not critical, to one (yellow points), which means that this point follows a power law and therefore is a candidate to a critical point. This figure shows a large extension of yellow points, mainly before the critical point of the original ZGB model,  $y \simeq 0.39$  (here named region 1). As can be seen, there is also a small region near the discontinuous point, around  $0.45 \lesssim y \lesssim 0.6$  and small values of  $k$ , which has a set of yellow points and looks like a tail (region 2). These behaviors can be easily explained: as the second order phase transition of the original model takes place at the point which separates the O poisoned phase from the beginning of the reactive state where the production of  $\text{CO}_2$  molecules starts, any value of  $k$  does not influence this transition substantially. However, for the discontinuous phase

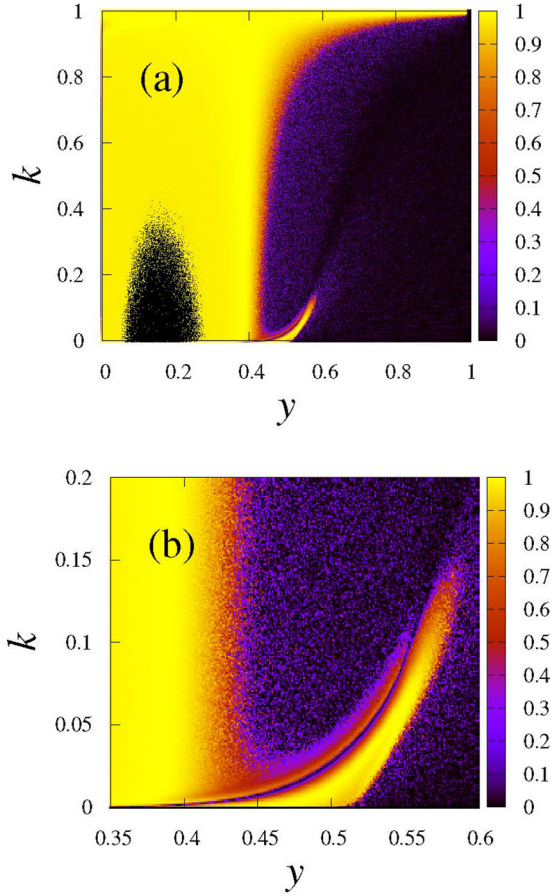


FIG. 1. (a) Coefficient of determination  $r$  as function of  $y$  and  $k$  for the ZGB model with desorption of CO molecules. (b) A highlight of the coefficient of determination  $r$  as function of  $y$  and  $k$  for the ZGB model with desorption of CO molecules. We can observe an extension that ends after the discontinuous phase transition point ( $y \approx 0.53$ ) of the model without desorption ( $k = 0$ ). This extension comes from continuous phase transition of the original ZGB model ( $y \approx 0.39$  and  $k = 0$ ).

transition this argument does not hold since at this point even a small value of  $k$  can avoid the poisoning of the surface with CO molecules, and, therefore,  $k$  substantially influences the transition to the point of eliminating the discontinuous phase transition.

In Fig. 1(b) we highlight the region that presents an extension coming from the continuous phase transition ( $y \approx 0.39$  and  $k = 0$ ) and that lasts up to  $y \approx 0.58$  and  $k \approx 0.15$ , which is close to the discontinuous phase transition of the original model  $y \approx 0.53$  and  $k = 0$ .

Before analyzing these two regions in detail, it is important to improve Fig. 1(a) in order to find points with best coefficients of determination. Figure 2 shows the refinement of Fig. 1(a) for higher values of  $r$ :  $r \geq 0.98$ ,  $0.99$ ,  $0.999$ , and  $0.9995$ . This figure shows a narrowing of the yellow points in both regions when one considers only  $r \geq 0.98$  to  $r \geq 0.9995$ . Figure 2(b) shows that, for  $r \geq 0.99$ , region 1 splits into two parts: the first one looks like an upside-down bow, and the second one is a straight vertical line which starts at  $y \approx 0.39$  and  $k = 0$  and increases to around  $k = 1$  when

two branches arise in both sides of the diagram. On the other hand, region 2 presents two well-defined lines which meet each other in  $y \sim 0.56$  and  $k \sim 0.07$ . A similar analysis can be done for  $r \geq 0.999$  [see Fig. 2(c)] with only a decrease of yellow points. So, as  $r \geq 0.999$  is a good value for the coefficient of determination, all these points can be considered as candidates to phase transition points. However, as we are looking for higher values of  $r$ , we consider in our study only values of  $r \approx 0.9995$  as presented in Fig. 2(d). This figure shows that region 1, around the critical adsorption rate of the original model ( $y \approx 0.39$ ) and for all values of  $k$ , is not affected by the desorption of CO molecules [49,53]. However, the discontinuous phase transition of the original ZGB model ( $y \approx 0.53$ ) and  $k \approx 0$  disappears even for very small values of  $k$  [46,53]. In this case, only few points appear in region 2.

In order to analyze these points, and more precisely the characteristics of their proximities, we consider the region  $0.44 \leq y \leq 0.56$  and  $0 \leq k \leq 0.09$  with the refinement  $r \geq 0.98$ , as shown in Fig. 3. As can be seen, this figure highlights the two curves presented in Fig. 2(a) which end in a given point. In order to characterize the phenomena related to this region we choose four values of  $y$ :  $0.530$ ,  $0.536$ ,  $0.542$ , and  $0.552$ , and calculate the coefficient of determination  $r$  for  $0 \leq k \leq 0.09$  with  $\Delta k = 0.001$ . The vertical dashed lines presented in Fig. 3(a) indicate where our analysis is performed. We can observe that three of these vertical lines cross both curves, which means a double peak in a plot of  $r$  versus  $k$  as shown in Fig. 3(b) for (i)  $y = 0.530$ , (ii)  $y = 0.536$ , and (iii)  $y = 0.542$ . However, the vertical line for  $y = 0.552$  [Fig. 3(a)] crosses the curve only once, i.e., there is only a single peak in Fig. 3(b) (iv). The inset plot in this figure corresponds only to a zoom, which indeed verifies the existence of a unique peak. As found in previous works [30,31], the two peaks are related to pseudocritical points (here interpreted from a nonequilibrium simulations' point of view) which characterize the discontinuous phase transitions (weak first order phase transitions). Here it is worth mentioning that in a previous work, Tomé and Dickman [46] found, for  $y = 0.54212$  and  $k = 0.0406$ , an critical adsorption rate associated with an Ising-like point. However, in our study, we believe that this point must be related to a single peak, as shown in the last plot of Fig. 3(b). According to our simulations the best candidate for this Ising-like point is slightly after  $y = 0.552$  and  $k = 0.064$ . In fact, our best value of the coefficient of determination,  $r = 0.99984$  was obtained for  $y = 0.554$  and  $k = 0.064$ .

At this point, two important questions arise: Is the narrow extension of points that grow up from  $k = 0$  to  $k = 1$  nearby  $y \approx 0.390$  critical? Is the point  $y = 0.554$  and  $k = 0.064$  an Ising-like critical point? If so, what can we say about its universality class?

In the next subsection, we carried out nonequilibrium MC simulations to look into several points of region 1 [Fig. 2(d)] in order to obtain some critical exponents. We also study the point corresponding to the best value of  $r$  of region 2,  $y = 0.554$  and  $k = 0.064$ , and obtain the dynamic critical exponent  $\theta$  to check for its universality class. However, region 2 deserves more attention, and, therefore, a more detailed study will be considered in an upcoming paper.

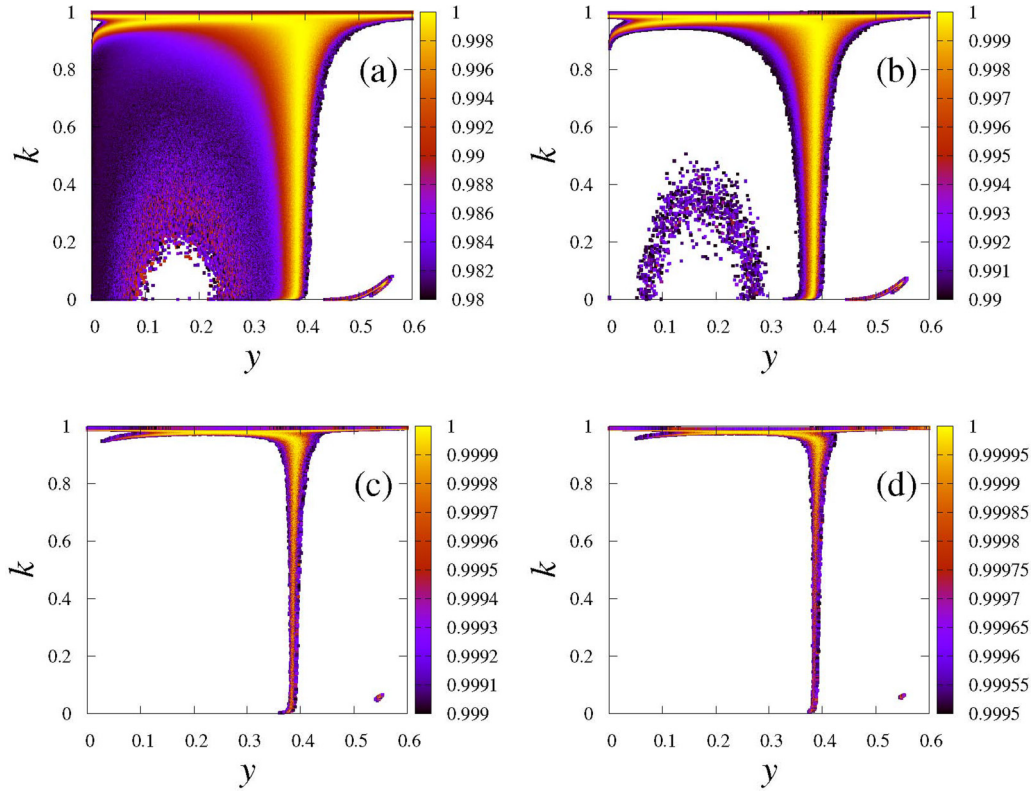


FIG. 2. Refinement process of the coefficient of determination for (a)  $r \geq 0.98$ , (b)  $r \geq 0.99$ , (c)  $r \geq 0.999$ , and (d)  $r \geq 0.9995$ .

### B. Critical exponents

In this subsection, we obtain the critical exponents  $\delta = \beta/\nu_{\parallel}$  and  $\theta$  of the model for some critical points of region 1, as well as the exponent  $\theta$  for a critical point of region 2, through nonequilibrium MC simulations in two-dimensional lattices. All results were obtained for the following set of parameters:  $L = 160$ ,  $N_{MC} = 300$ , and 5000 samples. The results are averages obtained through five different time evolutions and the error bars are obtained from them. To study region 1, we decided to consider some values of  $k$ , equally spaced and look for values of  $y_{best}$  which correspond to the best value of  $r_{best}$ . The values of  $k$ ,  $y_{best}$ , and  $r_{best}$  are shown in Table I. As shown in the second row of this table, the values of  $y$  are very close to the value of the critical adsorption rate of the original ZGB model,  $y = 0.388$ .

In order to obtain the critical exponents, we first consider the simulations starting with the initial condition  $\rho_0 = 0$ , i.e., where all sites of the lattice are initially occupied by CO molecules, and we also expect a power law described by Eq. (8). Figure 4(a) illustrates the time evolution of  $\rho(t)$  in log - log scale for one particular case:  $k = 0.1$  and  $y = 0.387$ . We can observe that after an initial transient,  $\rho(t)$  decays (the inset plot shows the corresponding linear fit in log - log scale). The error bars taken over five different seeds are indeed very small. The values obtained for  $\delta$  ( $\delta_{best}$ ) corresponding to the best  $y$  ( $y_{best}$ ) is relatively close to  $\delta = 0.451$  [41]. However, the results present a best are shown in the third row of Table I. The values are certainly a variation and do not permit us to assert that the points found in region 1 belong to the DP universality class. The values of the coefficient of determination for these points are presented in the fourth row of Table I.

Since the values of  $y$  (second row) are very close to  $y = 0.388$  (in fact, this value appears in four of the nine values presented in Table I), we also carried out simulations by considering the same values of  $k$  but kept  $y = 0.388$ . The coefficient of determination is still very close to 1, as shown in the sixth row of Table I, and the results for the exponent  $\delta$  are surprising. Now we have  $\delta$  even closer to the value of the DP universality class (see row five of the table).

Thus, our results suggest that the points of region 1 are critical ones and may belong to the DP universality class, but further studies must be performed in order to confirm (or disprove) this assertion. However, we have two more results to present in this work and which reinforce our previous estimates. First, we show the results related to the exponent  $\theta$ . Here it is important to note that the initial transient where  $\rho(t)$  increases before decaying as  $\rho(t) \sim t^{-\delta}$  does not correspond to the critical initial slip where the exponent  $\theta$  is usually obtained. In fact, this exponent is not expected for that initial condition. In addition, this initial transient lasts only for few steps (fewer than 10 MC steps). So we performed simulations for those same points presented in Table I with the initial condition where all sites are occupied by O atoms but a single site that remains vacant at the center of the lattice, i.e.,  $\rho_0 = 1/L^2$ . The time evolution of  $\rho(t)$  [given by Eq. (8)] is shown in Fig. 4(b). The gray lines introduced in this figure work as directions to observe that power laws are approximately parallel lines in log - log scale. The seventh row of Table I presents the exponents  $\theta$  for all considered points. These values are very close to  $\theta = 0.230$  found for the two-dimensional DP model [41]. The error bars are bigger for this initial condition as can also be

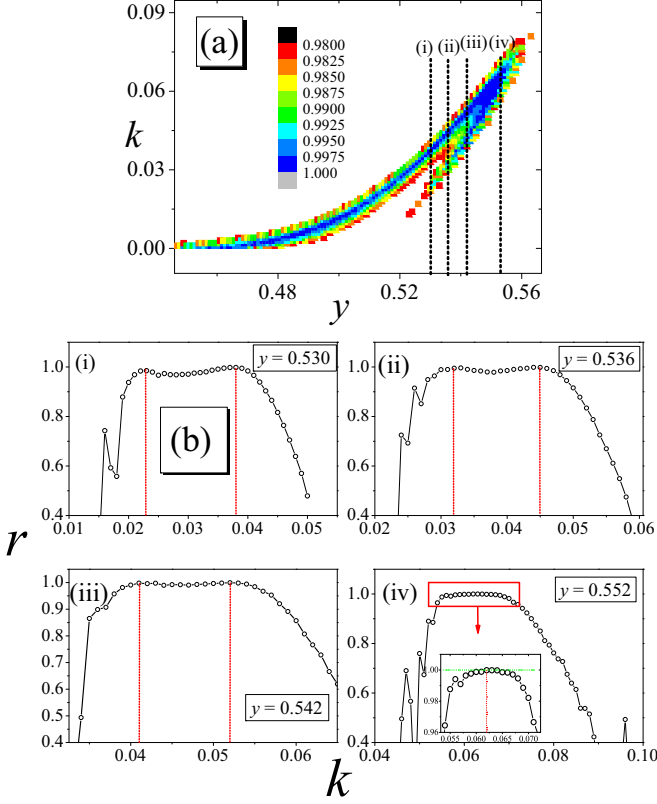


FIG. 3. (a) A small part of region 2 ( $0.44 \lesssim y \lesssim 0.56$  and  $k \lesssim 0.09$ ) corresponding to the two curves that, after the refinement, lead to a single point. The vertical dashed lines correspond to different values of  $y$ : (i)  $y = 0.530$ , (ii)  $y = 0.536$ , (iii)  $y = 0.542$ , and (iv)  $y = 0.552$ , where the coefficient of determination  $r$  is calculated as function of  $k$ . (b)  $r \times k$  for these values of  $y$ . We can observe that the double peaks observed in plots (i), (ii), and (iii) culminate in a single peak shown in plot (iv). The inset in plot (iv) is a zoom in order to verify the existence of a unique peak.

observed in Fig. 4(b) generating uncertainties in the second decimal digit.

Second, it is also possible to study the behavior of  $\rho(t) \sim t^{-\delta}$  when all initial sites are vacant, since we expect this behavior specifically for this initial condition when considering the density of vacant site as the order parameter of the model. We verified that, in this case, the exponent  $\delta$  corresponds exactly to what is expected when  $\rho_0 = 1$ , giving  $\delta \approx 0.45$  for all values of  $k$  as can be observed in Fig. 5, which present curves with approximately the same slope (parallel lines).

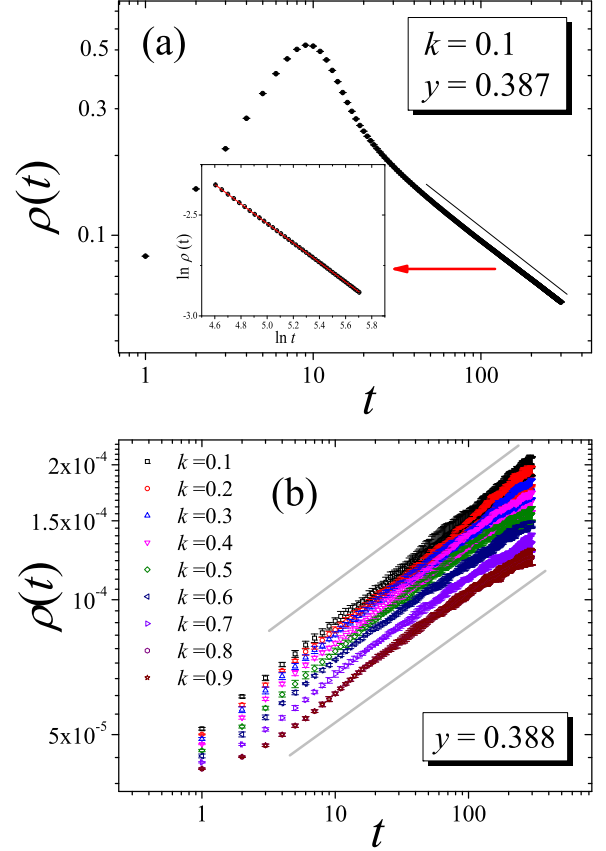


FIG. 4. (a) The time evolution of  $\rho(t)$  in log  $\times$  log scale for one particular case  $y = 0.387$  and  $k = 0.1$ , when all sites are initially filled with CO molecules. We can observe that after a transient, the system decays according to the power law given by Eq. (7) (the inset plot highlights the robustness of this power law). (b) The initial growing of  $\rho(t)$  when the initial lattice is fully occupied by O atoms except for a vacant site located at the center of the lattice. We show the power laws for  $k = 0.1, 0.2, \dots, 0.9$  and  $y = 0.388$ .

Since we unveiled region 1, let us briefly explore region 2, which, according to the previous subsection, culminates in a point corresponding to a unique peak for the coefficient of determination, after a succession of double peaks (pseudo-critical points). For this point ( $y_c = 0.554$  and  $k_c = 0.064$ ), we consider the initial lattice being fully occupied with CO molecules. Figure 6 shows the critical initial slip for the density of vacant sites as a function of  $t$ , in log-log scale.

TABLE I. Critical exponents estimated for the refined points of region 1.

$k$	0.1	0.2	0.3	0.4	0.5	0.6	0.7	0.8	0.9
$y_{\text{best}}$	0.387	0.388	0.387	0.388	0.391	0.388	0.391	0.390	0.392
$\delta_{\text{best}}$	0.4838(6)	0.4527(4)	0.4797(7)	0.4587(6)	0.4065(2)	0.4581(4)	0.4146(5)	0.4218(2)	0.3953(1)
$r_{\text{best}}$	0.999784	0.999767	0.999801	0.999867	0.999718	0.999928	0.999915	0.999953	0.999975
$\delta$	0.4532(3)	0.4527(3)	0.4546(4)	0.4587(6)	0.4587(5)	0.4581(4)	0.4515(4)	0.4396(5)	0.4153(3)
$r$	0.999770	0.999767	0.999650	0.999867	0.999541	0.999928	0.999898	0.999469	0.999829
$\theta$	0.24(1)	0.23(2)	0.23(2)	0.23(1)	0.22(1)	0.21(2)	0.21(1)	0.21(1)	0.21(1)

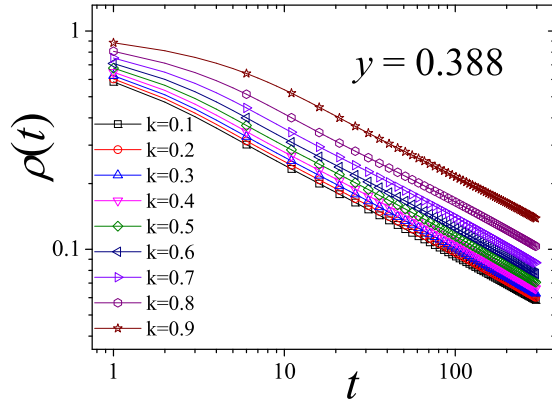


FIG. 5. Time evolution of  $\rho(t)$  for  $y = 0.388$  when we start with all sites vacant ( $\rho_0 = 1$ ) for  $k = 0.1, 0.2, \dots, 0.9$ .

The slope of this curve gives

$$\theta = 0.198(1), \quad (10)$$

and is in fair agreement with the results found for the Ising model,  $\theta \approx 0.193$  [3]. Our estimate identifies this critical point as belonging to the Ising universality class, exactly as predicted in Ref. [46] for the static exponent  $\nu$  for a point slightly before ours,  $y = 0.54212$  and  $k = 0.0406$ .

Actually, this is more general and deserves more comments. The kinetic Ising models, introduced by Glauber [67], have continuum generalizations described by the time-dependent Ginzburg-Landau theory. More precisely, there is a specific kinetic Ising universality class of the nonconserved order parameters, known as model A in the Halperin, Hohenberg, and Ma classification (see, for example, Ref. [68]). The universality class of kinetic Ising models also represents a large class of models that are intrinsically irreversible, i.e., without a defined Hamiltonian, such as all probabilistic cellular automata with “up-down” symmetry [69]. For example, Tomé and Oliveira [70] studied numerically the dynamic critical behavior of a family of nonequilibrium models with up-down symmetry: the Glauber model, majority vote model, and extreme model, obtaining  $\theta = 0.191(2)$ ,  $0.190(5)$ , and  $\theta = 0.188(8)$ , which is quite reasonable with the expected estimates.

It is important to notice that there is a class of models in the literature which presents a critical (bicritical) point which separates the model-A and directed-percolation critical lines. For instance, the nonequilibrium Potts model, whose dynamics has two absorbing states [71], belongs to the voter universality class [72]. In addition, the authors of Refs. [73–75] showed that the voter critical point is split in a transition that

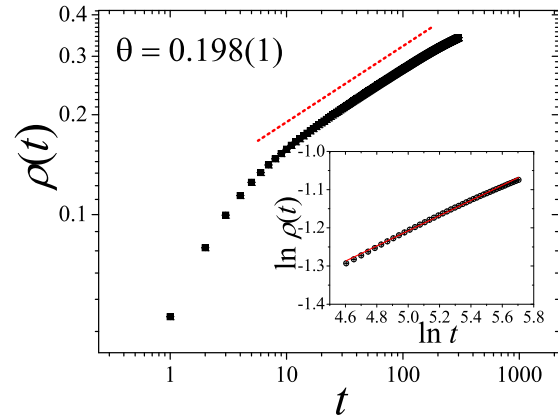


FIG. 6. Time evolution of density of vacant sites,  $\rho(t)$  vs  $t$ , for  $y = 0.554$  and  $k = 0.064$  when we start the simulation with all sites occupied by CO molecules.

belongs to the Ising universality class and the other one that belongs to DP universality class. This similarity between our model and this model that belongs to the voter universality class is not casual. For example, a generalized class of voter models, so-called generalized voter models [76], includes a particular case in the class of models of catalytic surfaces introduced by Swindle and Grannan [77]. Nonequilibrium studies of these similarities deserve future exploration.

#### IV. CONCLUSIONS

In this paper, we studied the ZGB model with desorption of CO molecules through nonequilibrium MC simulations and showed that it can belong to the DP and Ising universality classes depending on the values of the CO adsorption rate,  $y$ , and of the CO desorption rate,  $k$ . We presented the diagram  $k \times y$  obtained through the optimization of the coefficient of determination and showed that the region belonging to the DP universality class is composed of a line of critical points extending from  $0 \leq k \leq 1$  and  $y \simeq 0.388$ . The other region possesses two pseudocritical lines that probably intercept each other at the Ising-like critical point,  $y = 0.554$  and  $k = 0.064$ .

#### ACKNOWLEDGMENTS

This research work was in part supported financially by CNPq (National Council for Scientific and Technological Development). This work was partly developed using the resources of HPCC (High Performance Computer Center) Jataí. R.d.S. would like to thank L. G. Brunnet (IF-UFRGS) for kindly providing resources from Clustered Computing Center Ada Lovelace for the partial development of this work.

- [1] H. K. Janssen, B. Schaub, and B. Schmittmann, *Z. Phys. B* **73**, 539 (1989).  
 [2] D. A. Huse, *Phys. Rev. B* **40**, 304 (1989).  
 [3] B. Zheng, *Int. J. Mod. Phys. B* **12**, 1419 (1998).

- [4] B. Zheng and H. J. Luo, *Phys. Rev. E* **63**, 066130 (2001).  
 [5] E. V. Albano and M. A. Muñoz, *Phys. Rev. E* **63**, 031104 (2001).

- [6] R. da Silva, N. A. Alves, and J. R. Drugowich de Felício, *Phys. Lett. A* **298**, 325 (2002).
- [7] R. da Silva, N. A. Alves, and J. R. Drugowich de Felício, *Phys. Rev. E* **66**, 026130 (2002).
- [8] E. Arashiro and J. R. Drugowich de Felício, *Phys. Rev. E* **67**, 046123 (2003).
- [9] R. da Silva and J. R. Drugowich de Felício, *Phys. Lett. A* **333**, 277 (2004).
- [10] B. C. S. Grandi and W. Figueiredo, *Phys. Rev. E* **70**, 056109 (2004).
- [11] H. A. Fernandes, J. R. Drugowich de Felício, and A. A. Caparica, *Phys. Rev. B* **72**, 054434 (2005).
- [12] I. A. Hadjiagapiou, A. Malakis, and S. S. Martinos, *Physica A (Amsterdam)* **356**, 563 (2005).
- [13] H. A. Fernandes and J. R. Drugowich de Felício, *Phys. Rev. E* **73**, 057101 (2006).
- [14] H. A. Fernandes, E. Arashiro, J. R. Drugowich de Felício, and A. A. Caparica, *Physica A (Amsterdam)* **366**, 255 (2006).
- [15] H. A. Fernandes, R. da Silva, and J. R. Drugowich de Felício, *J. Stat. Mech.* (2006) P10002.
- [16] V. V. Prudnikov, P. V. Prudnikov, A. S. Krinitsyn, A. N. Vakilov, E. A. Pospelov, and M. V. Rychkov, *Phys. Rev. E* **81**, 011130 (2010).
- [17] R. da Silva, H. A. Fernandes, J. R. Drugowich de Felício, and W. Figueiredo, *Comput. Phys. Commun.* **184**, 2371 (2013).
- [18] R. da Silva, N. Alves Jr., and J. R. Drugowich de Felício, *Phys. Rev. E* **87**, 012131 (2013).
- [19] R. da Silva, H. A. Fernandes, and J. R. Drugowich de Felício, *Phys. Rev. E* **90**, 042101 (2014).
- [20] A. Chiochetta, A. Gambassi, S. Diehl, and J. Marino, *Phys. Rev. B* **94**, 174301 (2016).
- [21] H. A. Fernandes, R. da Silva, A. A. Caparica, and J. R. Drugowich de Felício, *Phys. Rev. E* **95**, 042105 (2017).
- [22] R. da Silva, J. R. Drugowich de Felício, and A. S. Martinez, *Phys. Rev. E* **85**, 066707 (2012).
- [23] E. Arashiro, J. R. Drugowich de Felício, and U. H. E. Hansmann, *Phys. Rev. E* **73**, 040902 (2006); *J. Chem. Phys.* **126**, 045107 (2007).
- [24] M.-B. Luo and C.-J. Qian, *Polymer* **47**, 1451 (2006).
- [25] R. da Silva, R. Dickman, and J. R. Drugowich de Felício, *Phys. Rev. E* **70**, 067701 (2004).
- [26] R. da Silva and H. A. Fernandes, *J. Stat. Mech.* (2015) P06011.
- [27] U. Basu, V. Volpati, S. Caracciolo, and A. Gambassi, *Phys. Rev. Lett.* **118**, 050602 (2017).
- [28] E. S. Loscar, C. G. Ferrara, and T. S. Grigera, *J. Chem. Phys.* **144**, 134501 (2016).
- [29] E. S. Loscar, D. A. Martin, and T. S. Grigera, *J. Chem. Phys.* **147**, 034504 (2017).
- [30] E. V. Albano, *Phys. Lett. A* **288**, 73 (2001).
- [31] H. A. Fernandes, R. da Silva, E. D. Santos, P. F. Gomes, and E. Arashiro, *Phys. Rev. E* **94**, 022129 (2016).
- [32] E. V. Albano, M. A. Bab, G. Baglietto, R. A. Borzi, T. S. Grigera, E. S. Loscar, D. E. Rodriguez, M. L. R. Puzzo, and G. P. Saracco, *Rep. Prog. Phys.* **74**, 026501 (2011).
- [33] J. W. Evans, *Langmuir* **7**, 2514 (1991).
- [34] E. V. Albano, *Surf. Sci.* **306**, 240 (1994).
- [35] M. F. de Andrade and W. Figueiredo, *Phys. Rev. E* **81**, 021114 (2010).
- [36] M. F. de Andrade and W. Figueiredo, *J. Chem. Phys.* **136**, 164502 (2012).
- [37] M. Ehsasi, M. Matlock, O. Frank, J. H. Block, K. Christmann, F. S. Rys, and W. Hirschwald, *J. Chem. Phys.* **91**, 4949 (1989).
- [38] K. Christmann, *Introduction to Surface Physical Chemistry* (Steinkopff Verlag, Darmstadt, 1991).
- [39] R. Imbhil and G. Ertl, *Chem. Rev.* **95**, 697 (1995).
- [40] R. M. Ziff, E. Gulari, and Y. Barshad, *Phys. Rev. Lett.* **56**, 2553 (1986).
- [41] C. A. Voigt and R. M. Ziff, *Phys. Rev. E* **56**, R6241 (1997).
- [42] R. M. Ziff and B. J. Brosilow, *Phys. Rev. A* **46**, 4630 (1992).
- [43] P. Meakin and D. J. Scalapino, *J. Chem. Phys.* **87**, 731 (1987).
- [44] R. Dickman, *Phys. Rev. A* **34**, 4246 (1986).
- [45] J. Marro and R. Dickman, *Nonequilibrium Phase Transitions in Lattice Models* (Cambridge University Press, Cambridge, 1999).
- [46] T. Tomé and R. Dickman, *Phys. Rev. E* **47**, 948 (1993).
- [47] P. Fischer and U. M. Titulaer, *Surf. Sci.* **221**, 409 (1989).
- [48] M. Dumont, P. Dufour, B. Sente, and R. Dagonnier, *J. Catal.* **122**, 95 (1990).
- [49] E. V. Albano, *Appl. Phys. A* **55**, 226 (1992).
- [50] B. J. Brosilow and R. M. Ziff, *Phys. Rev. A* **46**, 4534 (1992).
- [51] T. Matsushima, H. Hashimoto, and I. Toyoshima, *J. Catal.* **58**, 303 (1979).
- [52] G. M. Buendía and P. A. Rikvold, *Phys. Rev. E* **88**, 012132 (2013).
- [53] C. H. Chan and P. A. Rikvold, *Phys. Rev. E* **91**, 012103 (2015).
- [54] I. Jensen and H. C. Fogedby, *Phys. Rev. A* **42**, 1969 (1990).
- [55] H. P. Kaukonen and R. M. Nienimen, *J. Chem. Phys.* **91**, 4380 (1989).
- [56] G. M. Buendía and P. A. Rikvold, *Phys. A* **424**, 217 (2015).
- [57] B. C. S. Grandi and W. Figueiredo, *Phys. Rev. E* **65**, 036135 (2002).
- [58] G. L. Hoenicke and W. Figueiredo, *Phys. Rev. E* **62**, 6216 (2000).
- [59] G. M. Buendía and P. A. Rikvold, *Phys. Rev. E* **85**, 031143 (2012).
- [60] G. L. Hoenicke, M. F. de Andrade, and W. Figueiredo, *J. Chem. Phys.* **141**, 074709 (2014).
- [61] J. Satulovsky and E. V. Albano, *J. Chem. Phys.* **97**, 9440 (1992).
- [62] E. V. Albano, *Surf. Sci.* **235**, 351 (1990).
- [63] B. J. Brosilow, E. Gulari, and R. M. Ziff, *J. Chem. Phys.* **98**, 674 (1993).
- [64] K. S. Trivedi, *Probability and Statistics with Reliability, Queuing, and Computer Science and Applications*, 2nd ed. (John Wiley and Sons, Chichester, 2002).
- [65] J. W. Evans and M. S. Miesch, *Phys. Rev. Lett.* **66**, 833 (1991).
- [66] H. Hinrichsen, *Adv. Phys.* **49**, 815 (2000).
- [67] R. J. Glauber, *J. Math. Phys.* **4**, 294 (1963).
- [68] B. I. Halperin, P. C. Hohenberg, and S.-K. Ma, *Phys. Rev. B* **10**, 139 (1974); P. C. Hohenberg and B. I. Halperin, *Rev. Mod. Phys.* **49**, 435 (1977).
- [69] G. Grinstein, C. Jayaprakash, and Y. He, *Phys. Rev. Lett.* **55**, 2527 (1985).



- [70] T. Tomé and M. J. de Oliveira, *Phys. Rev. E* **58**, 4242 (1998).
- [71] A. Lipowski and M. Droz, *Phys. Rev. E* **65**, 056114 (2002).
- [72] I. Dornic, H. Chaté, J. Chave, and H. Hinrichsen, *Phys. Rev. Lett.* **87**, 045701 (2001).
- [73] M. Droz, A. L. Ferreira, and A. Lipowski, *Phys. Rev. E* **67**, 056108 (2003).
- [74] O. Al Hammal, H. Chaté, I. Dornic, and M. A. Muñoz, *Phys. Rev. Lett.* **94**, 230601 (2005).
- [75] A. L. Rodrigues, C. Chatelain, T. Tomé, and M. J. de Oliveira, *J. Stat. Mech.* (2015) P01035.
- [76] T. S. Mountford, *J. Stat. Phys.* **67**, 303 (1992).
- [77] E. Grannan and G. Swindle, *J. Stat. Phys.* **61**, 1085 (1990).